

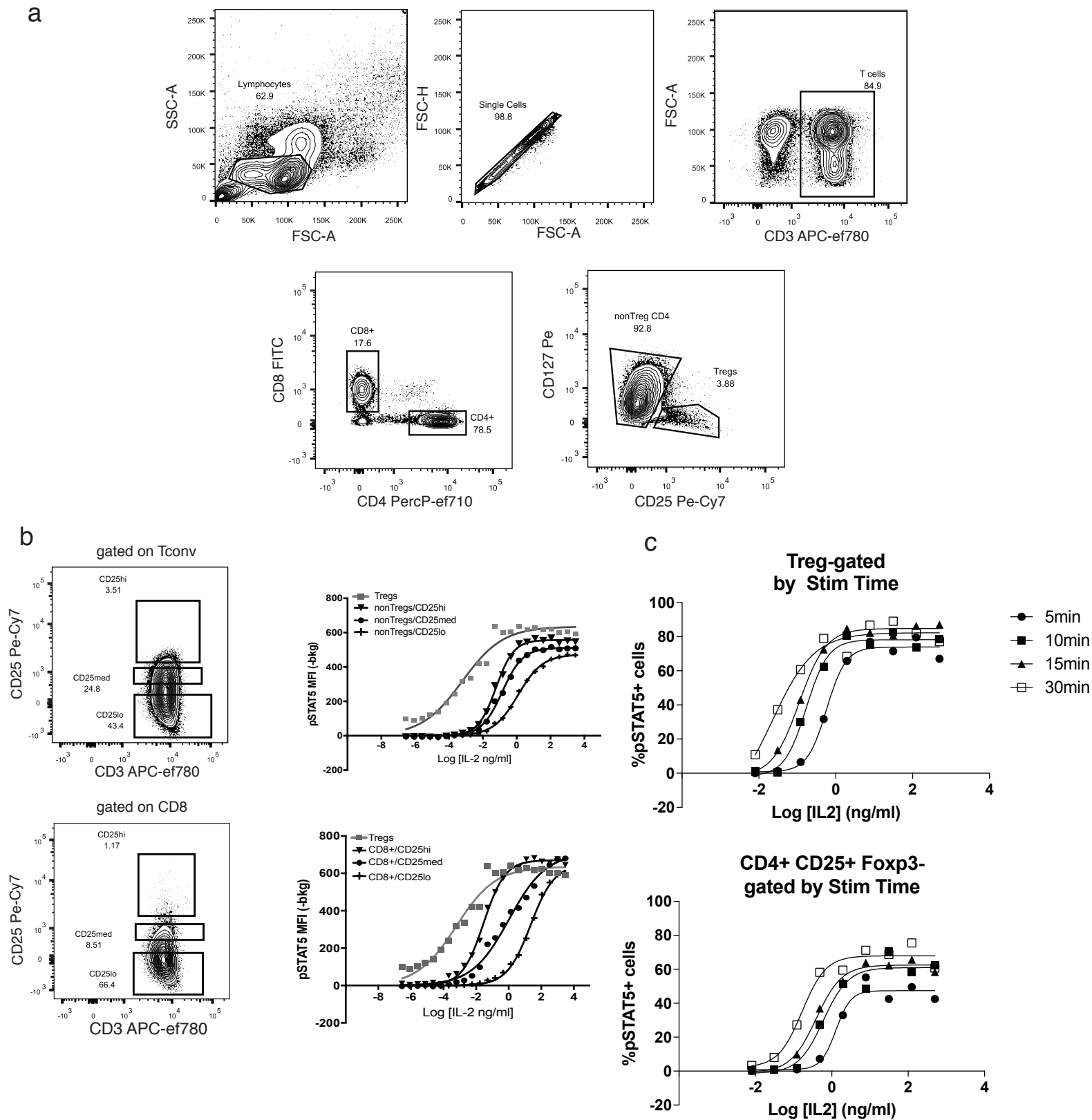
In the format provided by the authors and unedited.

# A human anti-IL-2 antibody that potentiates regulatory T cells by a structure-based mechanism

Eleonora Trotta<sup>1</sup>, Paul H. Bessette<sup>2</sup>, Stephanie L. Silveria<sup>1</sup>, Lauren K. Ely<sup>2</sup>, Kevin M. Jude<sup>3,4</sup>,  
Duy T. Le<sup>5</sup>, Charles R. Holst<sup>6</sup>, Anthony Coyle<sup>7</sup>, Marc Potempa<sup>8</sup>, Lewis L. Lanier<sup>8</sup>,  
K. Christopher Garcia<sup>3,4,9</sup>, Natasha K. Crellin<sup>2,11</sup>, Isaac J. Rondon<sup>2,11</sup> and Jeffrey A. Bluestone<sup>1,10,11\*</sup>

<sup>1</sup>UCSF Diabetes Center, University of California, San Francisco, San Francisco, CA, USA. <sup>2</sup>Centers for Therapeutic Innovation, Pfizer Inc., San Francisco, CA, USA. <sup>3</sup>Departments of Molecular & Cellular Physiology and Structural Biology, Stanford University, Stanford, CA, USA. <sup>4</sup>Stanford Cancer Institute, Stanford University School of Medicine, Stanford, CA, USA. <sup>5</sup>Department of Pediatric Immunology, Allergy and Rheumatology, University of Houston, Houston, TX, USA. <sup>6</sup>BioElectron Technology Corporation, Mountain View, CA, USA. <sup>7</sup>Pandion Therapeutics, Cambridge, MA, USA. <sup>8</sup>Department of Microbiology and Immunology, University of California, San Francisco, San Francisco, CA, USA. <sup>9</sup>Howard Hughes Medical Institute, Stanford University School of Medicine, Stanford, CA, USA. <sup>10</sup>Parker Institute for Cancer Immunotherapy, San Francisco, CA, USA. <sup>11</sup>These authors jointly supervised this work: Natasha K. Crellin, Isaac J. Rondon, Jeffrey A. Bluestone. \*e-mail: [Jeff.Bluestone@ucsf.edu](mailto:Jeff.Bluestone@ucsf.edu)

# Sup figure 1.

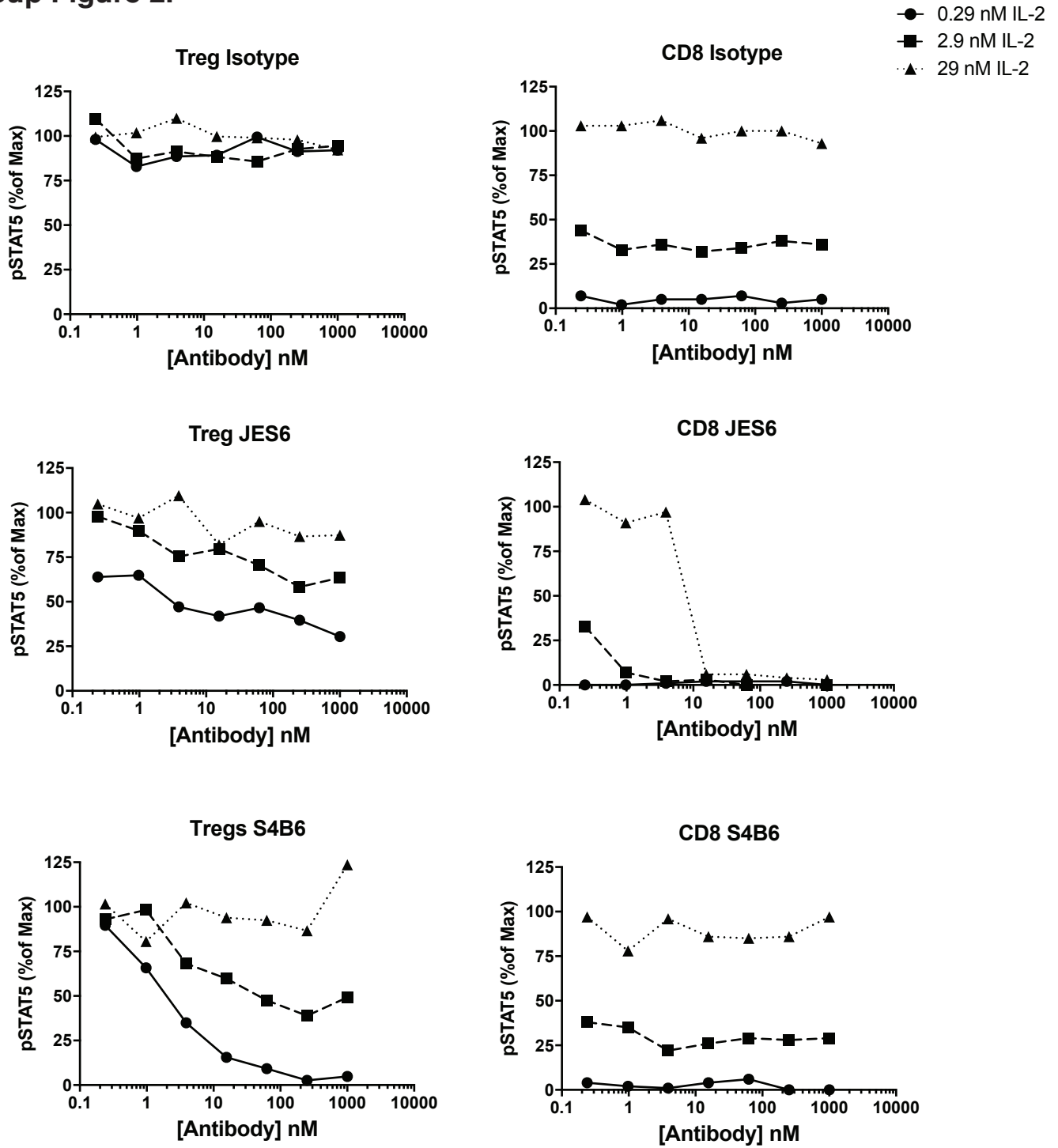


## Supplementary Figure 1: IL-2 sensitivity of different human T cells based on CD25 expression.

**(A)** pSTAT5 MFI of Tregs, CD4+ T cells and CD8+ T cells with different levels of CD25 expression in response to different concentrations of hIL-2. Representative flow plots of gating strategy for CD25lo, med and hi CD4+ T cells and CD8+ T cells. **(B)** Percentage of pSTAT5 Treg and Tconv cells in response to different hIL-2 concentrations at different time points. For A, cells were gated within PBMCs. For B, Treg and Tconv were FACS sorted and expanded using established protocols, and rested overnight without IL-2 prior to stimulation.

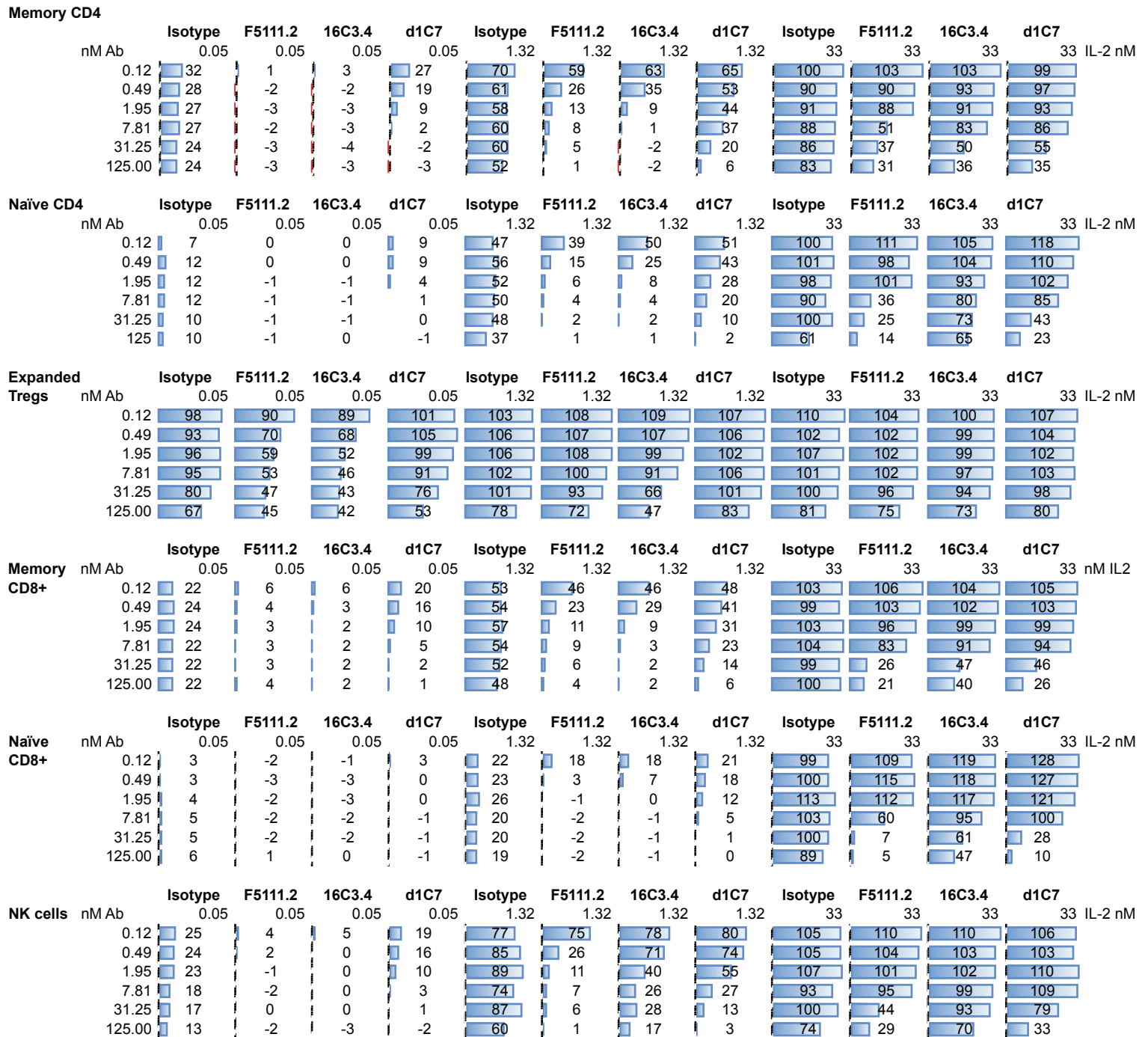


## Sup Figure 2.



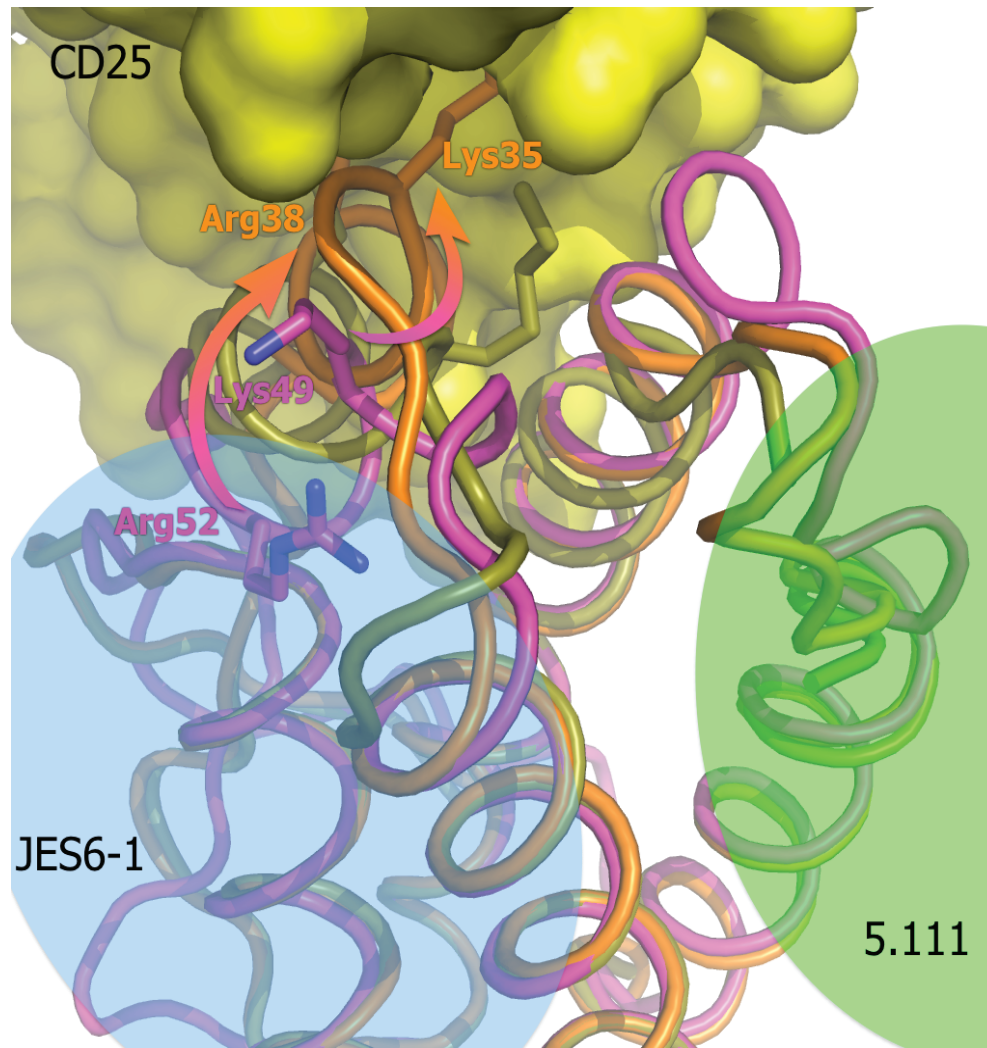
**Supplementary Figure 2. pSTAT5 signal profiling of mouse IL2: antibody complexes activity on fresh splenocytes.** Phosphorylation of STAT5 in mouse Tregs and CD8 phosphorylation in response to serial dilutions of JES6-1, S4B6 or isotype control Ig complexed with 1 of 3 different concentrations of mIL-2. Treg cells were identified by gating on CD4+ CD25+ FoxP3+ cells. The percent of pSTAT5 is normalized to the maximum IL-2 signal in the presence of the isotype control. Data are representative of 3 independent experiments

## Sup figure 3.



**Supplementary Figure 3. pSTAT5 signal profiling of IL-2:anti-IL-2 complex activity on isolated cell subsets.** Magnetic separation was used to isolate purified cell populations as labeled. Tregs were isolated by FACS sorting, and expanded ex vivo for 9 days prior to signaling assay. Serial dilutions of anti-hIL2 antibodies in complex with 1 of 3 different concentrations of hIL-2 (0.05nM, 1.3nM and 33nM) were used. A single donor representative of 3 is shown for each of the cell types.

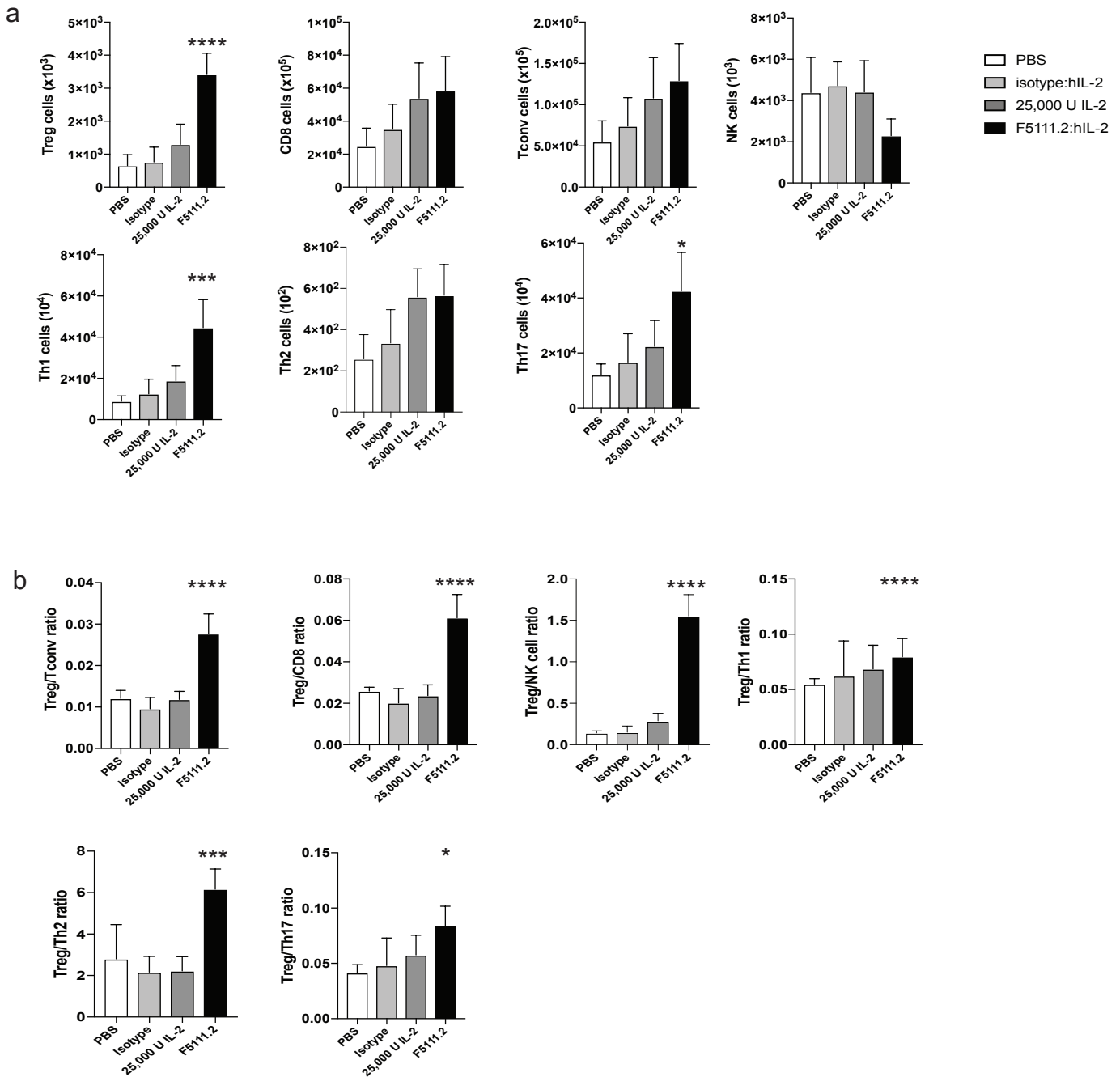
## Sup figure 4.



### Supplementary figure 4: F5111 and JES6-1 induce opposing allosteric structures of IL-2 at the CD25 binding site.

Structural alignment of hIL-2 from the IL-2:receptor quaternary complex (PDB ID 2B5I, olive), mIL-2 from the IL-2:JES6-1 complex (PDB ID 4YQX, magenta), and hIL-2 from the IL-2:F5111 complex (orange). Binding sites of JES6-1 and F5111 are depicted with blue and green shading, respectively. Relative movements between the JES6-1- and F5111-bound structures are illustrated with arrows.

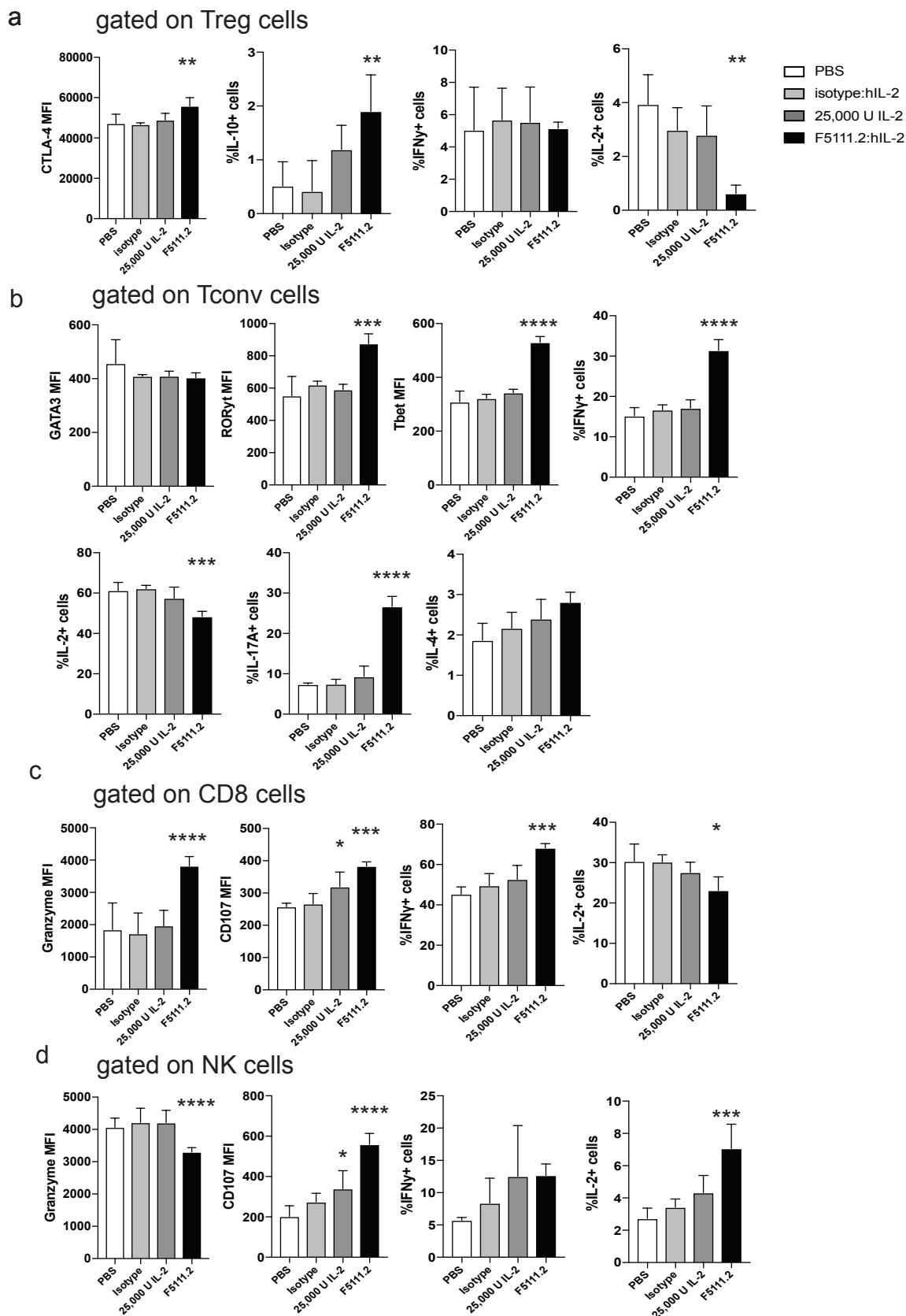
Sup figure 5.



**Supplementary Figure 5. Different immune populations after treatment with low dose IL-2 and F5111.2:hIL2 complexes in the NSG expansion model.**

(A) Treg, CD8, Tconv, NK, Th1, Th2, Th17 total cell number and (B) Treg/Tconv, Treg/CD8, Treg/NK cells, Treg/Th1, Treg/Th2, Treg/Th17 ratios after treatment with PBS, 25,000IU hIL-2, 25ug of F5111.2 and isotype in complex with 8,000U hIL-2. Data presented as a mean  $\pm$  s.d. of five mice per group. P values shown are determined by one-way ANOVA (Dunnett's multiple comparison test). \*  $P \leq 0.05$ , \*\*  $P \leq 0.01$ , \*\*\*  $P \leq 0.001$ , \*\*\*\*  $P \leq 0.001$

# Sup figure 6.

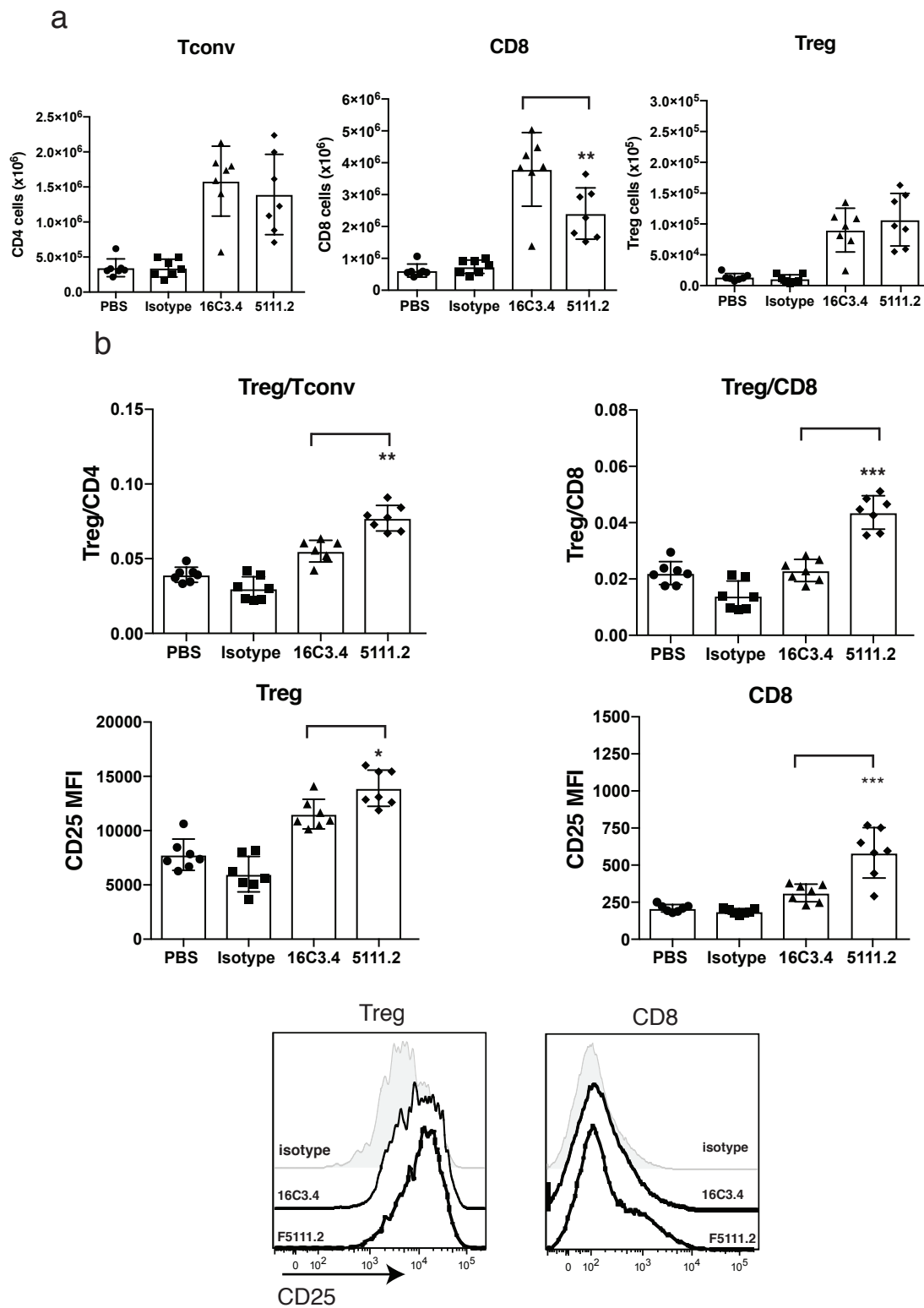


**Supplementary Figure 6. Cytokine production after treatment with low dose IL-2 and F5111.2:hIL2 complexes in the NSG expansion model.**

**(A)** CTLA-4 expression and percentage of IL10+, IFN $\gamma$  + and IL-2+ Tregs **(B)** GATA3, ROR $\gamma$ t, Tbet expression and percentage of IFN $\gamma$ +, IL-2+, IL-17A+ and IL-4+ Tconv cells. **(C)** Granzyme, CD107 expression and percentage of IFN $\gamma$ +, IL-2+ CD8+ T cells and NK cells. Data presented as a mean  $\pm$  s.d. of five mice per group. P values shown are determined by one-way ANOVA (Dunnnett's multiple comparison test)

\* P  $\leq$  0.05, \*\* P  $\leq$  0.01, \*\*\* P  $\leq$  0.001, \*\*\*\* P  $\leq$  0.001

## Sup figure 7.

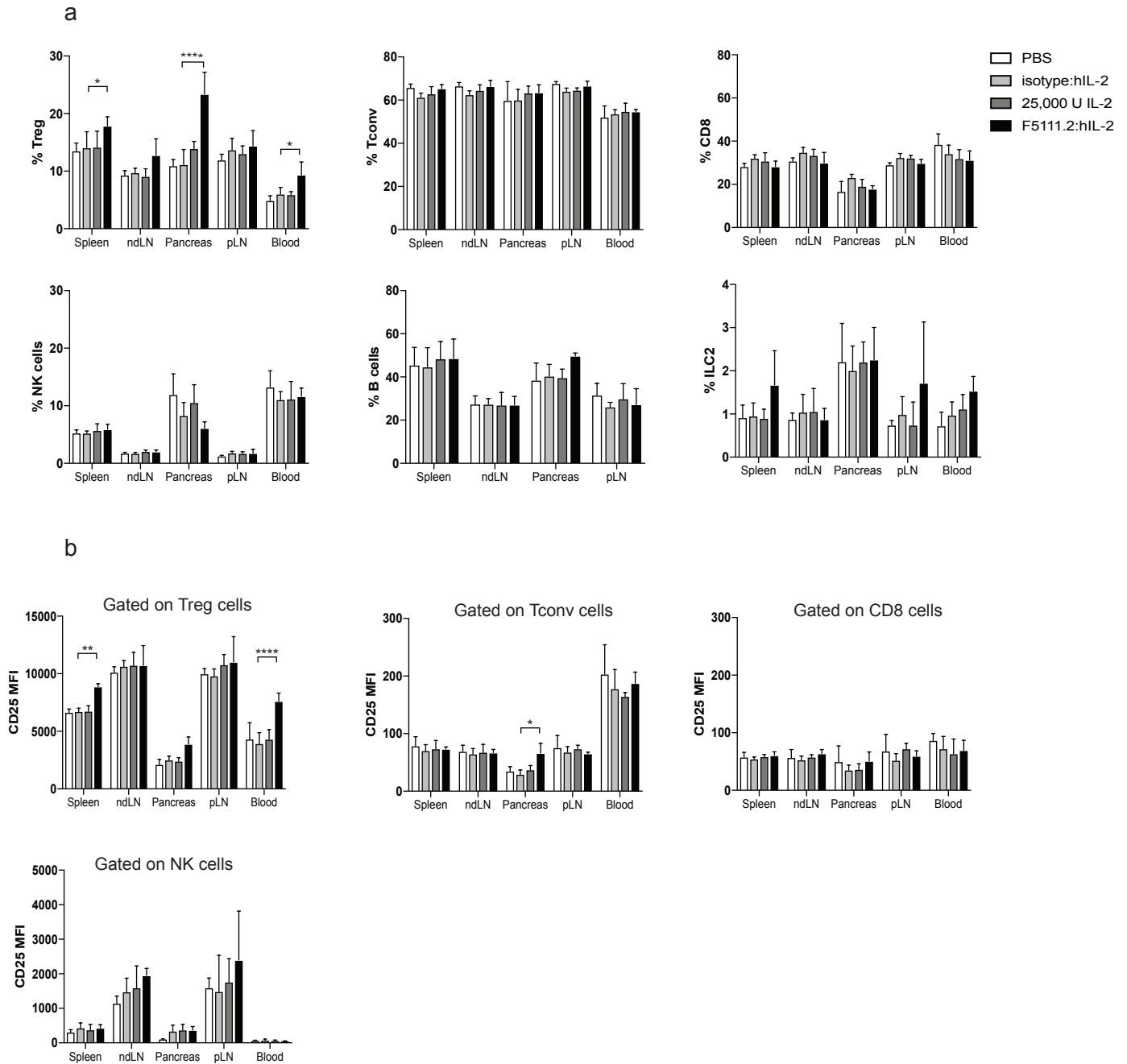


### Supplementary figure 7: F5111.2:hIL-2 complex treatment increases Tregs more than complete IL-2R $\alpha$ blocker 16C3.4:hIL-2 in vivo.

(A) Tconv, CD8<sup>+</sup> T and Treg total cell numbers (B) Treg/Tconv, Treg/CD8 ratios and (C) CD25 MFI expression on Treg and CD8<sup>+</sup> T cells after 5 consecutive days treatment with PBS or hIL-2 in complex with isotype (25 $\mu$ g), 16C3.4 (25 $\mu$ g), or F5111.2 (25 $\mu$ g). One of 3 experiments is shown, with data presented as a mean  $\pm$  s.d. of 7 mice per group.

P values shown are determined by one-way ANOVA (Dunnett's test). \*  $P \leq 0.05$ , \*\*  $P \leq 0.01$ , \*\*\*  $P \leq 0.001$ .

## Sup figure 8.



### Supplementary Figure 8: Different immune populations after treatment with low dose IL-2 and F5111.2:hIL2 complex in NOD mice.

Twenty-two week-old female NOD mice were treated with daily injections of PBS, 25,000IU hIL-2, 25 $\mu$ g of F5111.2 and isotype in complex with 8,000U hIL-2 for five consecutive days.

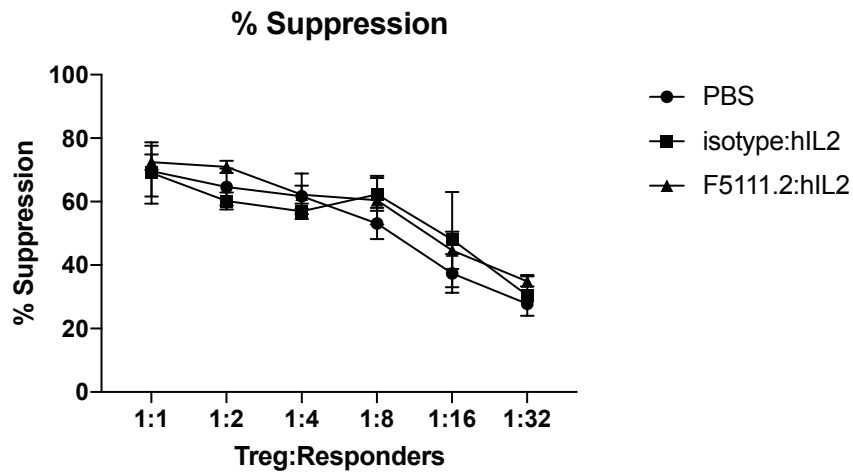
**(A)** Percentage of Treg, Tconv, CD8+ T, NK, B and ILC2 cells and **(B)** CD25 expression on Tregs, Tconv, CD8+ T and NK cells in spleen, non-draining lymph node (LN), pancreas, pancreatic LN and blood.

Data presented as a mean  $\pm$  s.d. of 4 mice per group.

P values shown are determined by one-way ANOVA (Dunnett's test). \*  $P \leq 0.05$ , \*\*  $P \leq 0.01$ , \*\*\*  $P \leq 0.001$ .

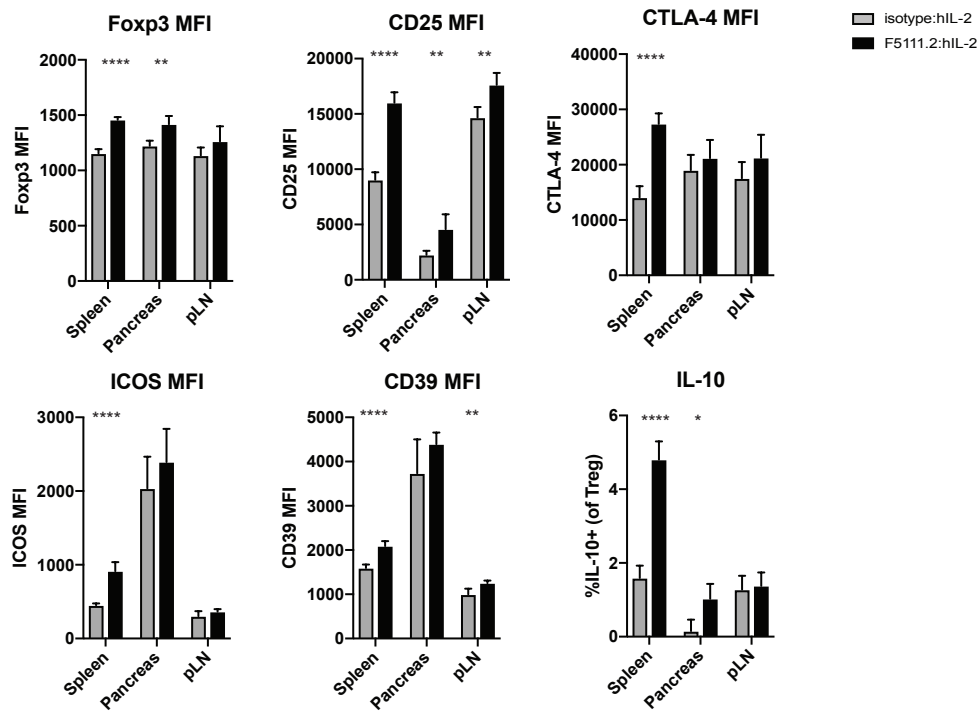
# Sup figure 9.

a

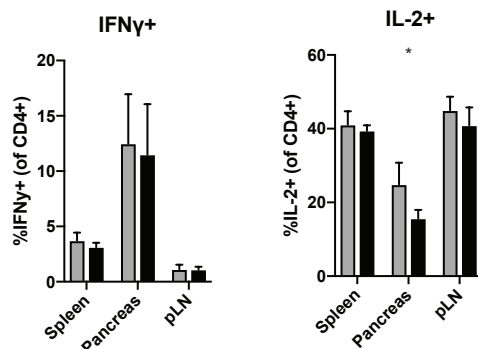


b

Gated on Treg



Gated on CD4+ cells



## Supplementary Figure 9: Suppression ability of Tregs expanded in response to F5111.2:hIL-2 complex.

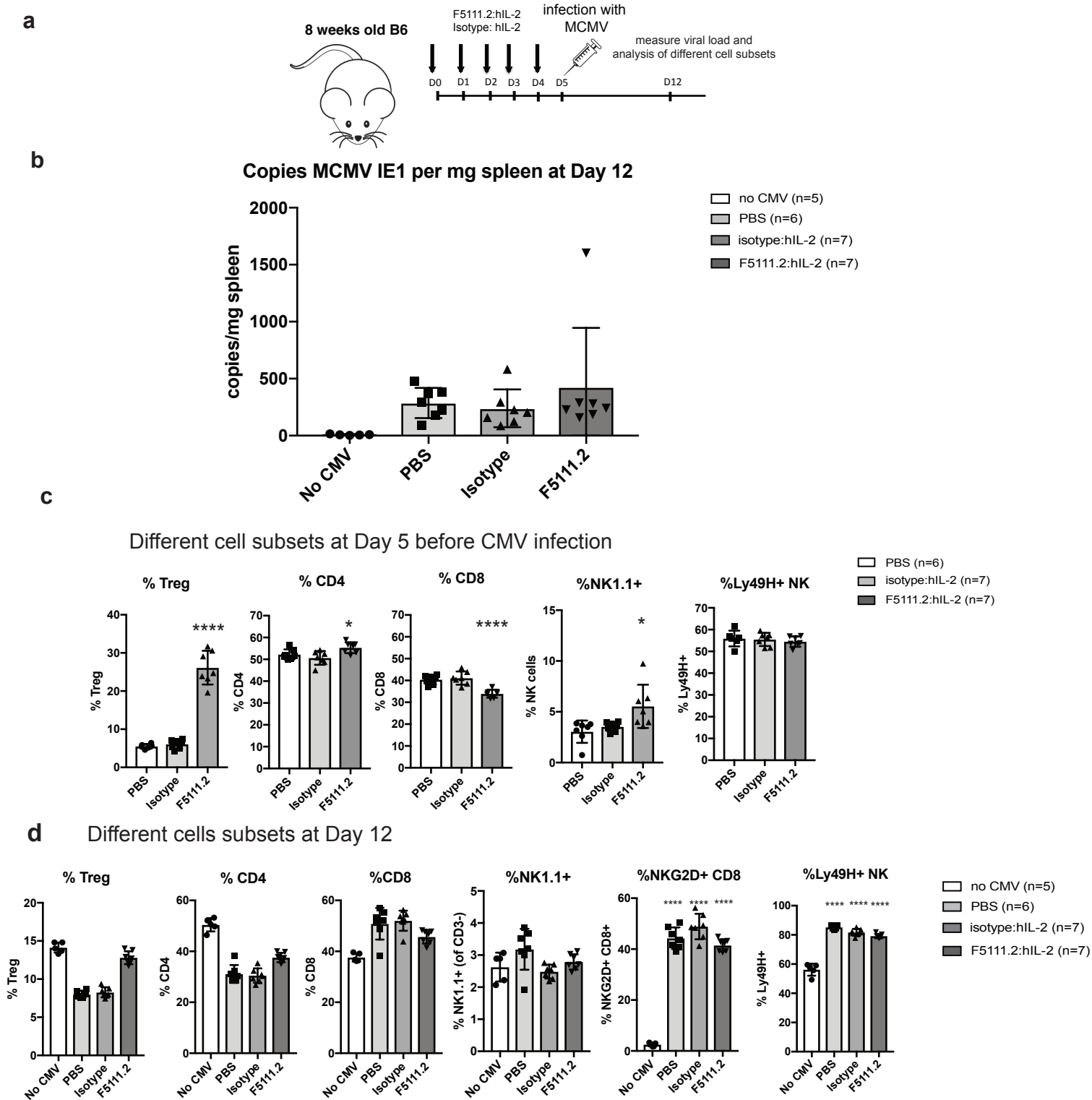
Twenty-two week-old female NOD mice were treated with daily injections of PBS, 125 $\mu$ g of F5111.2 and isotype in complex with 8,000U hIL-2 for five consecutive days. Tregs, naïve Teff and APC were isolated and used for suppression assay (A) The plot shows percent suppression with titrating levels of Tregs. Data presented as a mean  $\pm$  s.d. of triplicate wells. (B) FoxP3, CD25, CTLA-4, ICOS, CD39 expression, percentage of IL-10+ Tregs and IFN $\gamma$ +, IL-2+ CD4+ T cells. Data presented as a mean  $\pm$  s.d. of five mice per group.

P values shown were determined by a two-tailed paired Student's t-test and 95% confidence intervals.

\* P  $\leq$  0.05, \*\* P  $\leq$  0.01



## Sup figure 10.



### Supplementary Figure 10: F5111.2:IL-2 complex treatment doesn't affect the de novo generation of MCMV- specific NKG2D+ CD8+ T cells or Ly49H+ NK cells.

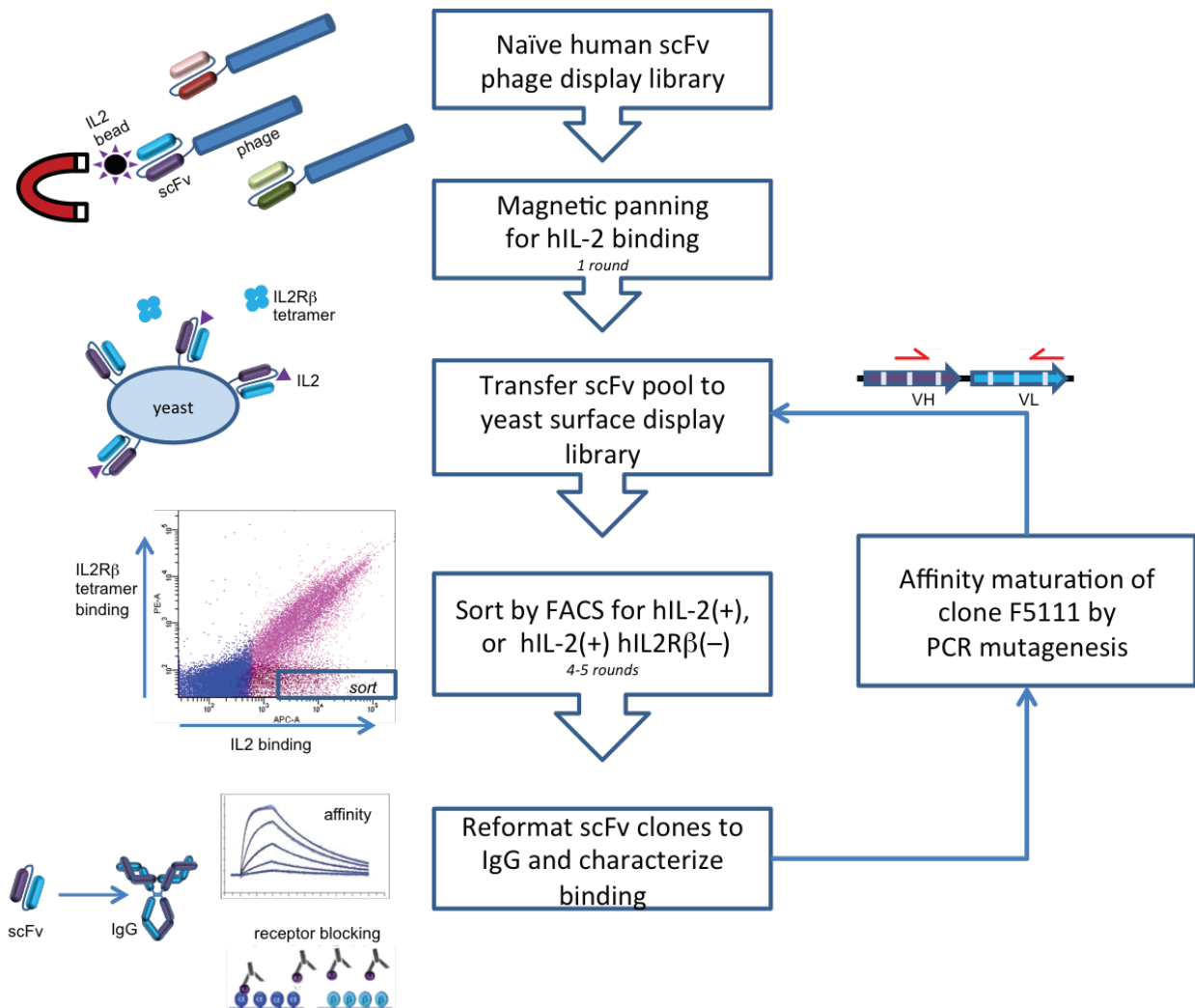
(A) 8 weeks old B6 mice were treated with daily injections of 25ug of F5111.2 and isotype in complex with 8,000U hiL-2 for five consecutive days. (B) Percentage of Tregs, CD4, CD8, NK1.1+ cells and Ly49H+ NK cells was assessed at Day 5 in the blood after treatment with F5111.2:hiL-2 complex and before MCMV infection and (C) at Day 12 in the spleen. Gating strategy shown in Supplementary Figure 14.

(D) Copies of MCMV IE1 per mg spleen. Data presented as a mean  $\pm$  s.d of five mice per group.

P values shown are determined by one-way ANOVA (Dunnett's multiple comparison test)

\*  $P \leq 0.05$ , \*\*  $P \leq 0.01$ , \*\*\*  $P \leq 0.001$ , \*\*\*\*  $P \leq 0.001$

## Sup figure 11.



### Supplementary Figure 11. Anti-IL-2 antibodies generation.

Anti-IL-2 scFvs were selected from a phagemid-based naive human library displayed on M13 bacteriophage. Selection was based on phage binding to biotinylated human IL-2 immobilized on streptavidin-coated magnetic beads. Human IL-2 was fused on its N-terminus with a 6-histidine purification tag, expressed transiently in HEK293 mammalian cell culture, purified by Ni-NTA affinity chromatography, and chemically biotinylated with EZ-Link NHS-PEG4-Biotin (Thermo Pierce). After one round of phage-display selection, the output pool of scFv genes was sub-cloned to a yeast surface display vector, and further rounds of sorting were conducted by fluorescent activated cell-sorting (FACS) after solution phase binding to biotinylated IL-2 and secondary fluorescent conjugates. In order to bias the antibody epitope towards the IL-2R $\beta$ -binding site on IL-2, alternate rounds of sorting included soluble IL-2R $\beta$  fluorescent tetramers in addition to IL-2, and IL-2R $\beta$  positive events were discarded. Subsequently, scFv genes were sequenced from yeast clones and reformatted to IgG1 with reduced effector function for expression in HEK293 cells (Invitrogen). Antibody F5111 was affinity matured by yeast display and FACS. Soft randomized degenerate oligonucleotides were used to mutate CDR2 of the heavy chain and CDR3 of the light chain, and the resulting library was sorted for high affinity by equilibrium or kinetic competition binding.

# Sup. Table 1

**Table 1 Data collection and refinement statistics**

| F5111 Fab – IL-2                                     |                               |
|--|-------------------------------|
| <b>Data collection</b>                               |                               |
| Wavelength (Å)                                       | 0.99988                       |
| Space group  | P 1 21 1                      |
| Cell dimensions                                      |                               |
| <i>a</i> , <i>b</i> , <i>c</i> (Å)                   | 86.01, 145.73, 107.32         |
| $\alpha$ , $\beta$ , $\gamma$ (°)                    | 90, 95.38, 90                 |
| Resolution (Å)                                       | 2.747                         |
| <i>R</i> <sub>sym</sub> or <i>R</i> <sub>merge</sub> | 0.1472 (1.356)                |
| <i>I</i> / $\sigma I$                                | 8.44 (0.84)                   |
| Completeness (%)                                     | 98.87 (95.08)                 |
| Redundancy   | 3.3 (3.2)                     |
| <b>Refinement</b>                                    |                               |
| Resolution (Å)                                       | 86.17 – 2.747 (2.845 – 2.747) |
| No. reflections                                      | 224403 (20815)                |
| <i>R</i> <sub>work</sub> / <i>R</i> <sub>free</sub>  | 0.1911/ 0.2472                |
| No. atoms  | 17680                         |
| Protein  | 17325                         |
| Ligand/ion   | 24                            |
| Water  | 331                           |
| <i>B</i> -factors                                    | 58.40                         |
| Protein  | 58.70                         |
| Ligand/ion   | 69.00                         |
| Water  | 42.90                         |
| Ramachandran Plot                                    |                               |
| Favored (%)  | 98.0                          |
| Outliers (%)   | 0.045                         |
| R.m.s. deviations                                    |                               |
| Bond lengths (Å)                                     | 0.002                         |
| Bond angles (°)                                      | 0.66                          |

\*Values in parentheses are for highest-resolution shell.